Thermodynamic limits for assimilation of silicate crust in primitive magmas

Jussi S. Heinonen[1]*, Frank J. Spera[2] and Wendy A. Bohrson[3]
[1]Department of Geosciences and Geography, University of Helsinki, P.O. Box 64, 00014 Helsinki, Finland
[2]Department of Earth Science and Institute for Crustal Studies, University of California, Santa Barbara, California 93106, USA
[3]Department of Geology and Geological Engineering, Colorado School of Mines, Golden, Colorado 80401, USA

ABSTRACT

Some geochemical models for basaltic and more primitive rocks suggest that their parental magmas have assimilated tens of weight percent of crustal silicate wall rock. But what are the thermodynamic limits for assimilation in primitive magmas? We pursue this question quantitatively using a freely available thermodynamic tool for phase equilibria modeling of open magmatic systems—the Magma Chamber Simulator (https://mcs.geol.ucsb.edu)—and focus on modeling assimilation of wall-rock partial melts, which is thermodynamically more efficient compared to bulk assimilation of stoped wall-rock blocks in primitive igneous systems. In the simulations, diverse komatiitic, picritic, and basaltic parental magmas assimilate progressive partial melts of preheated average lower, middle, and upper crust in amounts allowed by thermodynamics. Our results indicate that it is difficult for any subalkaline primitive magma to assimilate more than 20–30 wt% of upper or middle crust before evolving to compositions with higher SiO_2 than a basaltic magma (52 wt%). On the other hand, typical komatiitic magmas have thermodynamic potential to assimilate as much as their own mass (59–102 wt%) of lower crust and retain a basaltic composition. The compositions of the parental melt and the assimilant heavily influence both how much assimilation is energetically possible in primitive magmas and the final magma composition given typical temperatures. These findings have important implications for the role of assimilation in the generation and evolution of, e.g., ultramafic to mafic trans-Moho magmatic systems, siliceous high-Mg basalts, and massif-type anorthosites.

INTRODUCTION

Magmatic assimilation of crustal materials has important consequences for magma differentiation and crustal growth. Assimilation induces the formation of ore deposits (e.g., Hayes et al., 2015; Samalens et al., 2017) and affects the volatile budget and evolution of volcanic systems (e.g., Dallai et al., 2011; Rivera et al., 2017). It is also effective in masking primary incompatible trace element and isotopic signatures of mantle-derived magmas (e.g., Carlson et al., 1981; Lightfoot et al., 1990; Moore et al., 2020). Studying mantle sources and mantle versus crustal contributions of magmatic systems therefore requires an understanding of assimilation processes.

Much of the modeling of assimilation has been based on binary mixing and assimilation–fractional crystallization (AFC) equations (e.g., DePaolo, 1981) that rely solely on trace element and isotopic data. These methods may be useful in providing tentative information, but they do not inform the modeler about the associated changes in phase equilibrium or whether the results are reasonable in terms of energy conservation. Incompatible and compatible trace element concentrations in bulk assimilant may be magnitudes lower or higher, respectively, than in associated partial melts. Accordingly, amounts of crustal assimilation in excess of 30 wt% (relative to the initial magma) have been implied for basaltic or more primitive magmas by such models (e.g., Carlson et al., 1981; Lightfoot et al., 1990; Larsen and Pedersen, 2009). Is it possible for primitive magmas to assimilate such high amounts of silicate crust or its partial melts? Would the contaminated magmas remain basaltic?
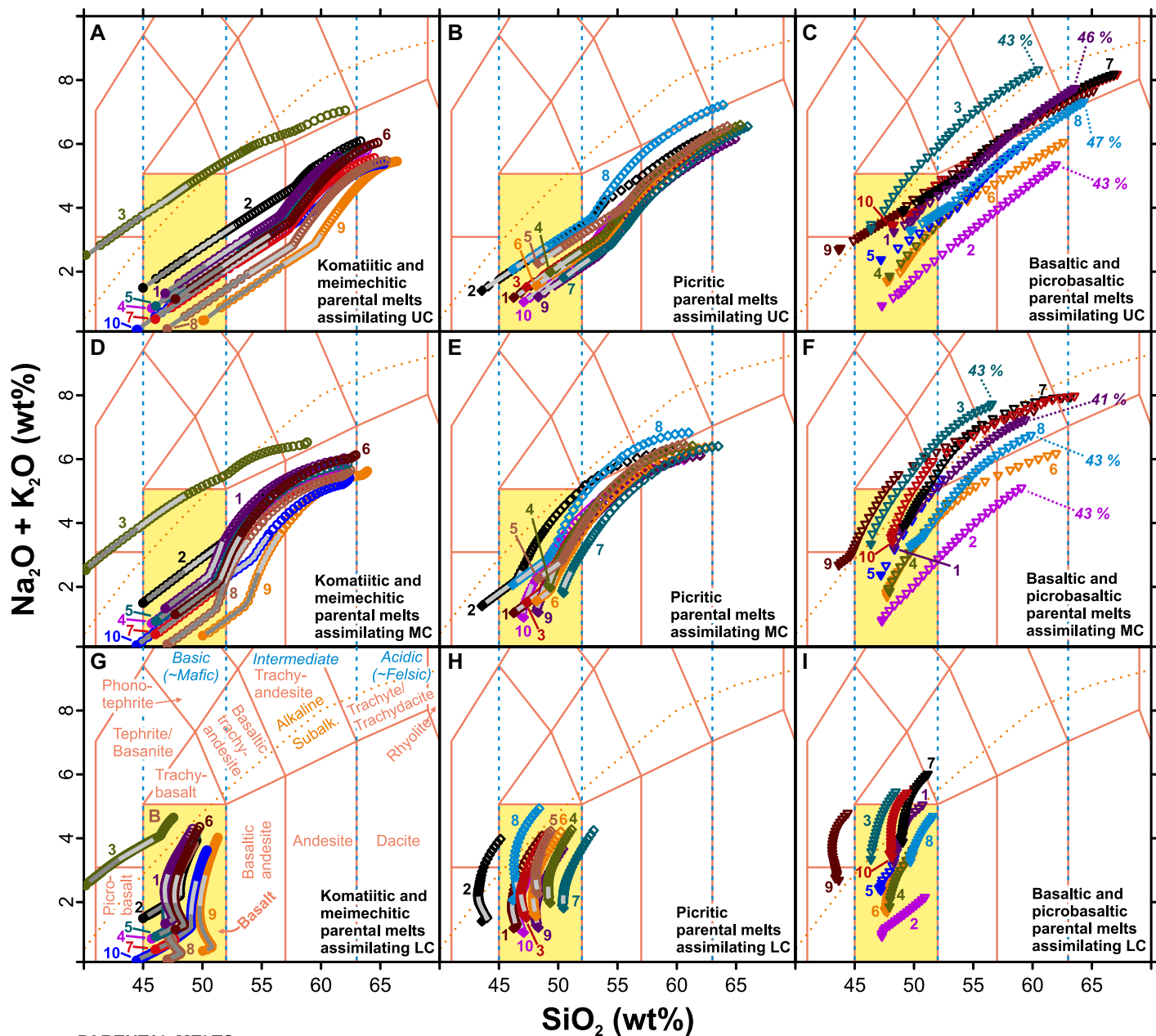
In this study, we quantitatively test thermodynamic limits for assimilation in primitive magmas using the Magma Chamber Simulator (MCS, https://mcs.geol.ucsb.edu; Bohrson et al., 2014, 2020). MCS is a freely available open-system thermodynamic model that computes the thermal, mass, and compositional evolution of a multicomponent-multiphase composite system using a selected MELTS (http://melts.ofm-research.org) engine (here rhyolite-MELTS version 1.2.0; Gualda et al., 2012; Ghiorso and Gualda, 2015). The rhyolite-MELTS algorithms are suitable for modeling phase equilibria in multicomponent magmatic systems, and they generally provide reasonable first-order results when compared to natural and experimental data not used in their calibration (e.g., Hirschmann et al., 1998; Pamukcu et al., 2015; Pichavant et al., 2019). In the thermodynamically constrained AFC simulations presented here, komatiitic, picritic, and basaltic magmas assimilate progressive partial melts of average lower crust (LC), middle crust (MC), and upper crust (UC). This approach builds on earlier, more rudimentary models (e.g., Sparks, 1986; Thompson et al., 2002) and enables direct thermodynamic evaluation of how much assimilation of silicate-crust partial melt is possible by primitive crystallizing magmas before they evolve to intermediate to felsic compositions.

MODELING WITH MAGMA CHAMBER SIMULATOR

In MCS, assimilation can be modeled as assimilation of wall-rock partial melts–fractional crystallization (MCS-AFC) or assimilation of stoped blocks–fractional crystallization (MCS-SFC), or their combination (Bohrson et al., 2020). For the purpose of searching for thermodynamic limits of assimilation, attention is focused on MCS-AFC because MCS-SFC results in higher amounts of crystallization in the parent magma. This is because the added crystalline mass is of lower specific enthalpy

*E-mail: jussi.s.heinonen@helsinki.fi

Figure 1. Results of Magma Chamber Simulator (https://mcs.geol.ucsb.edu) simulations of assimilation of wall-rock partial melts–fractional crystallization (MCS-AFC) shown in SiO_2 versus $Na_2O + K_2O$ (total alkalis–silica, TAS) diagrams (Le Bas et al., 1986; basalt field highlighted in yellow). (A,D,G) Komatiitic and meimechitic parental melts (MgO >18 wt%; SiO_2 <52 wt%, alkalis not considered). (B,E,H) Picritic parental melts (MgO ≈ 12–18 wt%; SiO_2 <52 wt%, alkalis not considered). (C,F,I) Basaltic and picrobasaltic parental melts (MgO <12 wt%; SiO_2 <52 wt%; $Na_2O + K_2O$ <5 wt%) (Le Bas et al., 1986; Le Bas, 2000). Parental melt locations and sources are given in Table S1 (see footnote 1). Each open symbol represents assimilation step where wall-rock partial melt above percolation threshold of 10 wt% is homogenized with resident melt. Dark and light gray trendlines highlight high-Mg compositions (komatiitic or meimechitic and picritic in terms of MgO, respectively) outside of TAS classification (see Fig. 2). Only results with <50 wt% crystallinity of resident magma are shown. Stippled lines and numbers in italics in C and F indicate total amount of assimilation (in weight percent relative to initial parental melt) in end of simulations using arc parental melts 1, 2, 3, and 8. UC, MC, LC—upper, middle, and lower crust, respectively; Subalk.—subalkaline; LIP—large igneous province; GB—greenstone belt; MORB—mid-oceanic ridge basalt; CFB—continental flood basalt; MEI—meimechitic; FP—ferropicritic.

compared to partial melt of the same composition and temperature (see the Discussion section, and the Supplemental Material[1]).

Input for MCS-AFC scenarios includes pressure, initial temperature, wall-rock melt percolation threshold, and the relative mass of the magma and the wall rock and their respective major element compositions. Additionally, thermal input parameters for modeling the behavior and phase equilibria of the wall rock at near-solidus conditions are required. For a thorough explanation of the model input, see Bohrson et al. (2020). In an MCS-AFC model, the sensible and latent heat released by crystallizing magma heats and partially melts the wall rock. After the amount of partial melt in the wall rock exceeds a percolation threshold, portions of wall-rock melt above this threshold are assimilated by the magma. The simulation proceeds until the magma and wall rock reach thermal equilibrium.

Full listings of the compositional input as well as discussion and sources for the model parameters can be found in the Supplemental Material. The 30 selected parental komatiitic or meimechitic, picritic, and picrobasaltic or basaltic parental melts represent different ages and tectonic settings (Fig. 1). The more magnesian parental melts are relevant to high-temperature Archean and large-igneous-province settings, whereas less magnesian parental melts are relevant to modern arc and other settings not related to mantle plumes. Water has been added to some of the compositions reported as dry, and initial Fe_2O_3/ FeO has been estimated based on constraints relevant to each setting and composition. The wall-rock compositions represent the average modern LC (basaltic andesite; $SiO_2 = 53$ wt%), MC (dacitic; $SiO_2 = 63$ wt%), and UC (dacitic; $SiO_2 = 66$ wt%) of Rudnick and Gao (2003). The mass of wall rock in the simulations is set at twice that of the initially pristine primitive magmas. To maximize assimilation, the initial temperature of the wall rock is slightly hypersolidus such that wall rock contained melt but was below the approximated percolation threshold of 10 wt% melt (LC: 9.4 wt% melt at 1060 °C and 0.8 GPa; MC: 9.7 wt% melt at 880 °C and 0.5 GPa; UC: 6.9 wt% melt at 700 °C and 0.2 GPa). Such conditions would approximate tabular chambers and high magma input having caused earlier crustal heating and steep geotherms prior to the intrusion of the modeled magma batch.

RESULTS OF THE MODELING

The results of the 90 (30 parental melts at 3 crustal settings) MCS-AFC simulations are illustrated in total alkalis–silica diagrams in Figure 1 and in histograms in Figure 2. The full output with additional preliminary models can be found in the Supplemental Material. Simulations using LC and UC assimilants present end-member scenarios among the presented simulations—simulations using a MC assimilant show transitional characteristics but are very much reminiscent of the UC cases in general.

It is unlikely for any primitive parental melt to assimilate more than 20−30 wt% (relative to the mass of the parental melt) of MC or UC before evolving to compositions with higher SiO_2 than basalts (52 wt%) (Fig. 2). Basaltic parental melts also cannot assimilate LC in excess of 20−30 wt% and remain basaltic. On the other hand, komatiitic parental melts have thermodynamic potential to assimilate as much as their own mass of LC (range of 59−102 wt%) and remain basaltic. Even picritic parental melts, relevant to Phanerozoic intraplate settings, can assimilate 28−49 wt% of LC before surpassing the SiO_2 content of basalts. Assimilation of LC partial melts can also increase the alkalinity of the magma series, which is more unlikely to be realized by assimilation of relatively more Si-rich MC or UC melts (Fig. 1).

DISCUSSION

A rather clear energetic limit exists for assimilation of anatectic melts of granitic crust by basaltic or more MgO-rich and SiO_2-poor magmas. Traditional binary mixing or AFC models that rely on trace elements and radiogenic
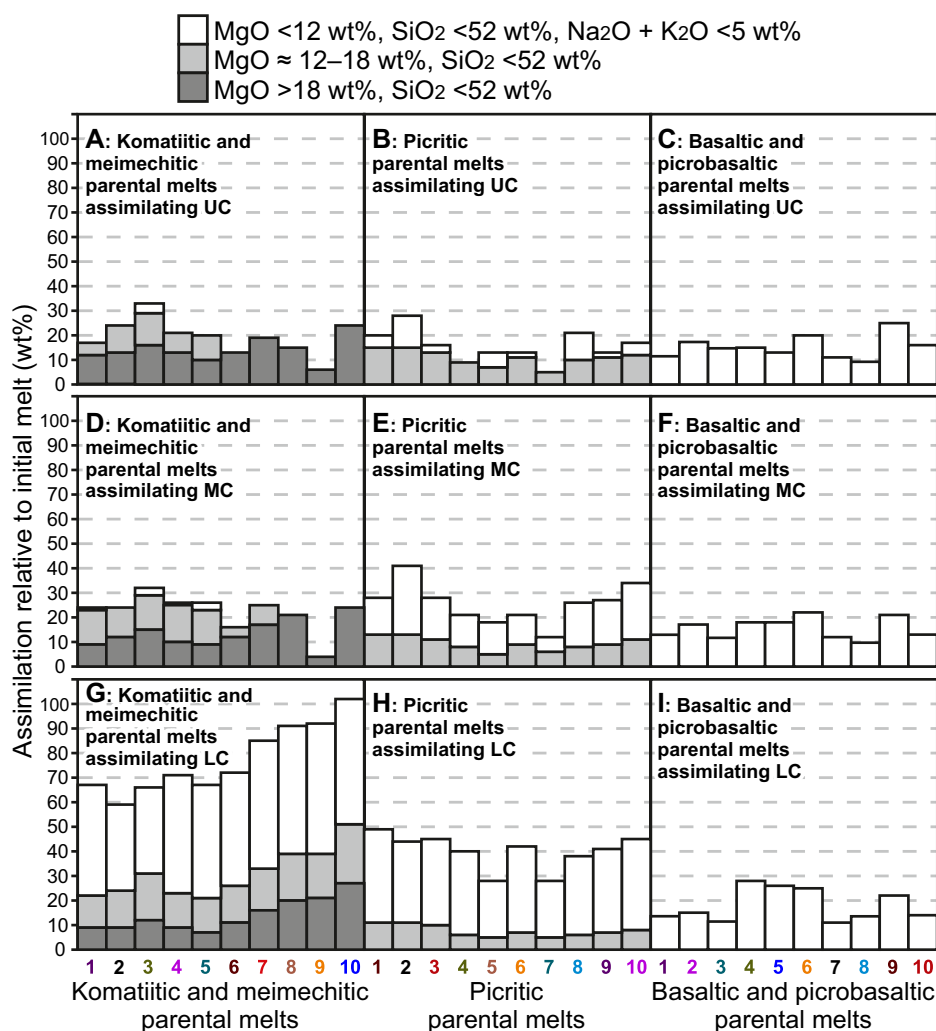

Figure 2. Results of Magma Chamber Simulator (https://mcs.geol.ucsb.edu) simulations of assimilation of wall-rock partial melts–fractional crystallization (MCS-AFC) shown in histograms. (A,D,G) Komatiitic and meimechitic parental melts. (B,E,H) Picritic parental melts. (C,F,I) Basaltic and picrobasaltic parental melts. See Figure 1 for more details and numbering of parental melts on horizontal axis. Vertical axes denote amount of assimilation relative to mass of parental melt. Amounts of assimilation in models are shown for three categories, where modeled resident melt composition can be considered komatiitic or meimechitic, picritic, or basaltic (see Fig. 1) and is below <50 wt% of crystallinity of resident magma. Numerical data used to construct this figure are tabulated in Table S2 (see footnote 1). UC, MC, LC—upper, middle, and lower crust, respectively.
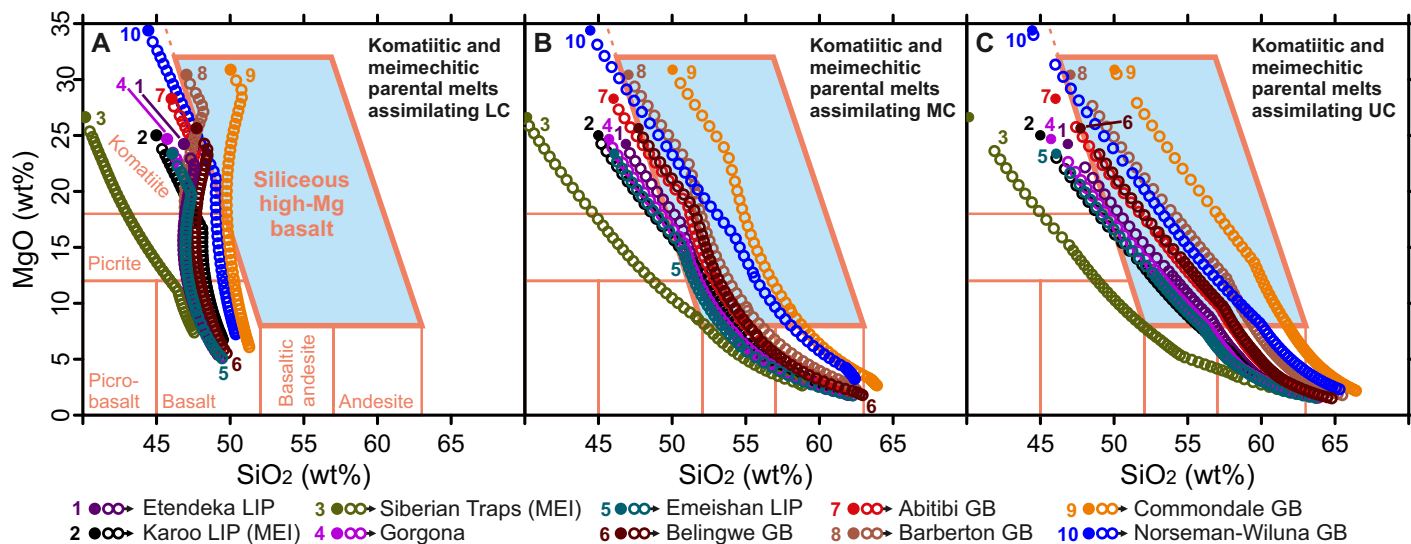
Figure 3. Results of Magma Chamber Simulator (https://mcs.geol.ucsb.edu) simulations of assimilation of wall-rock partial melts–fractional crystallization (MCS-AFC) for komatiitic-meimechitic parental melts shown in SiO_2 versus MgO diagrams overlain with relevant portions of boninite classification of Pearce and Reagan (2019). Maximum amounts of assimilation for modeled magmas that entered siliceous high-Mg basalt field (highlighted in blue) are 4–25 wt% (average = 15 wt%, $n = 4$) in A, 35–60 wt% (average = 43 wt%, $n = 10$) in B, and 34–48 wt% (average = 39 wt%, $n = 9$) in C. See Figure 1 for abbreviations and model details.

isotopes and suggest more than ~20−30 wt% assimilation of granitoid crust in primitive komatiitic, picritic, or basaltic systems are not broadly supported by the modeling (Figs. 1 and 2). For example, compositions produced by notable amounts of assimilation of felsic crust by komatiitic magmas correspond to siliceous high-Mg basalts and not komatiites or picrites (Fig. 3; see also Sparks, 1986; Pearce and Reagan, 2019). Our results underline the importance of considering thermodynamics and phase equilibria before attempting to model trace elements and isotopes in magmatic systems.

In contrast to the UC cases, the thermodynamic potential of komatiitic and picritic magmas to partially melt and assimilate LC and still retain primitive Si-poor compositions is considerable. This may have fundamental importance for how trans-Moho magmatic systems evolve. Examples include mineralization related to large-scale melting-infiltration fronts (e.g., Barnes et al., 2020) and generation of massif-type anorthosites and associated mafic rocks with geochemical evidence of considerable element input from (lower) crustal sources (e.g., Sparks, 1986; Heinonen et al., 2010; Bybee and Ashwal, 2015). Such magmatic systems may be easier to explain with a more dominant role for LC and its partial melts in their evolution than previously realized, and we encourage future thermodynamically constrained studies on these issues.

The presented modeling is also directly linked to fundamental research questions concerning the growth versus reworking of continental crust through time and in various geological settings (e.g., Hawkesworth et al., 2019). For example, modern arc basalts cannot assimilate more than 10−20 wt% of crustal

materials and remain basaltic (basaltic parental melts 1, 2, 3, and 8 in Fig. 2). For LC assimilation scenarios, basaltic parental melts cannot even evolve to considerably more SiO_2-rich compositions before assimilation halts due to thermal equilibrium reached with the mafic LC wall rock (Fig. 1I). Subsequent differentiation in such lower-crustal chambers would thus take place via fractional crystallization. For MC and UC assimilation scenarios, however, the magmas evolve to andesitic-dacitic compositions while assimilating >40 wt% of crustal materials (Figs. 1C and 1F). These constraints may be relevant for studies that concentrate on the differentiation of arc magmas, e.g., within the framework of melting-assimilation-storage-homogenization (MASH; Hildreth and Moorbath, 1988) scenarios. We encourage the future use of MCS to place thermodynamic constraints on assimilation also in more evolved systems.

The prerequisites for maximum degrees of assimilation are that the crust has been preheated by earlier magma pulses (or the geotherm is otherwise anomalously steep) and that the partial melts are effectively transported and mixed with the resident melt. It is well known that dynamic factors such as boundary-layer fractionation (e.g., Trial and Spera, 1990; Kuritani et al., 2005) may significantly inhibit the latter. In alternative models of bulk assimilation (e.g., reactive bulk assimilation; Beard et al., 2005), the crystallinity in the magma more readily reaches ~50 wt% due to the "enthalpy deficit" induced by incorporation of solid rather than partial melt, thus raising magma viscosity and potentially transforming magma to a semi-rigid crystal network rheologically incapable of subsequent large-scale differentiation (see Glazner,

2007). This feature is also shown by our comparative MCS-SFC simulations (see the Supplemental Material) that otherwise show similar results to the MCS-AFC simulations. In all the MCS-AFC results discussed here, the crystallinity of the resident magma stays <50 wt%.

Although reactive bulk assimilation may play an important role in the evolution of some low-temperature intermediate-felsic magmas (Beard et al., 2005), the considerable thermodynamic potential of ultramafic-mafic magmas to partially melt crustal materials (Figs. 1 and 2) suggests that the latter may dominate the style of assimilation in primitive magmatic systems (see also Kvassnes and Grove, 2008; Borisova et al., 2017). We nevertheless consider the amounts of partial-melt assimilation suggested by our simulations to represent absolute maximum values for natural settings—it is indeed very likely that other physical factors, not considered in our thermodynamic modeling, prevent assimilation in magma systems before the full thermodynamic potential of the intruding magmas has been harnessed. Thermodynamic models, as presented here, provide a framework into which additional kinetic and dynamic constraints can be placed to study natural systems in more detail.

It is also noteworthy that the computations presented in this study, especially in terms of the crustal assimilants, represent common and average compositions—these results are thus not directly applicable to scenarios involving rarer magma types or wall rock (e.g., ultrapotassic or carbonate compositions) or involving magma–wall rock interaction dominated by processes other than assimilation of wall-rock partial melts (e.g., selective metasomatism; Dyer et al., 2011). In spite of these shortcomings, we believe that

the results provide valuable insight into the energetic capabilities of primitive magmas in various geologic environments.

REFERENCES CITED
Barnes, S.J., Taranovic, V., Miller, J.M., Boyce, G., and Beresford, S., 2020, Sulfide emplacement and migration in the Nova-Bollinger Ni-Cu-Co deposit, Albany-Fraser Orogen, western Australia: Economic Geology and the Bulletin of the Society of Economic Geologists, v. 115, p. 1749–1776, https://doi.org/10.5382/econgeo.4758.

Beard, J.S., Ragland, P.C., and Crawford, M.L., 2005, Reactive bulk assimilation: A model for crust-mantle mixing in silicic magmas: Geology, v. 33, p. 681–684, https://doi.org/10.1130/G21470AR.1.

Bohrson, W.A., Spera, F.J., Ghiorso, M.S., Brown, G.A., Creamer, J.B., and Mayfield, A., 2014, Thermodynamic model for energy-constrained open-system evolution of crustal magma bodies undergoing simultaneous recharge, assimilation and crystallization: The Magma Chamber Simulator: Journal of Petrology, v. 55, p. 1685–1717, https://doi.org/10.1093/petrology/egu036.

Bohrson, W.A., Spera, F.J., Heinonen, J.S., Brown, G.A., Scruggs, M.A., Adams, J.V., Takach, M.K., Zeff, G., and Suikkanen, E., 2020, Diagnosing open-system magmatic processes using the Magma Chamber Simulator (MCS): Part I—Major elements and phase equilibria: Contributions to Mineralogy and Petrology, v. 175, 104, https://doi.org/10.1007/s00410-020-01722-z.

Borisova, A.Y., Bohrson, W.A., and Grégoire, M., 2017, Origin of primitive ocean island basalts by crustal gabbro assimilation and multiple recharge of plume-derived melts: Geochemistry Geophysics Geosystems, v. 18, p. 2701–2716, https://doi.org/10.1002/2017GC006986.

Bybee, G.M., and Ashwal, L.D., 2015, Isotopic disequilibrium and lower crustal contamination in slowly ascending magmas: Insights from Proterozoic anorthosites: Geochimica et Cosmochimica Acta, v. 167, p. 286–300, https://doi.org/10.1016/j.gca.2015.07.034.

Carlson, R.W., Lugmair, G.W., and MacDougall, J.D., 1981, Columbia River volcanism: The question of mantle heterogeneity or crustal contamination: Geochimica et Cosmochimica Acta, v. 45, p. 2483–2499, https://doi.org/10.1016/0016-7037(81)90100-9.

Dallai, L., Cioni, R., Boschi, C., and D'Oriano, C., 2011, Carbonate-derived CO_2 purging magma at depth: Influence on the eruptive activity of Somma-Vesuvius, Italy: Earth and Planetary Science Letters, v. 310, p. 84–95, https://doi.org/10.1016/j.epsl.2011.07.013.

DePaolo, D.J., 1981, Trace element and isotopic effects of combined wallrock assimilation and fractional crystallization: Earth and Planetary Science Letters, v. 53, p. 189–202, https://doi.org/10.1016/0012-821X(81)90153-9.

Dyer, B., Lee, C.-T.A., Leeman, W.P., and Tice, M., 2011, Open-system behavior during pluton–wall-rock interaction as constrained from a study of endoskarns in the Sierra Nevada Batholith, California: Journal of Petrology, v. 52, p. 1987–2008, https://doi.org/10.1093/petrology/egr037.

Ghiorso, M.S., and Gualda, G.A.R., 2015, An H_2O–CO_2 mixed fluid saturation model compatible with rhyolite-MELTS: Contributions to Mineralogy and Petrology, v. 169, 53, https://doi.org/10.1007/s00410-015-1141-8.

Glazner, A.F., 2007, Thermal limitations on incorporation of wall rock into magma: Geology, v. 35, p. 319–322, https://doi.org/10.1130/G23134A.1.

Gualda, G.A.R., Ghiorso, M.S., Lemons, R.V., and Carley, T.L., 2012, Rhyolite-MELTS: A modified calibration of MELTS optimized for silica-rich, fluid-bearing magmatic systems: Journal of Petrology, v. 53, p. 875–890, https://doi.org/10.1093/petrology/egr080.

Hawkesworth, C., Cawood, P.A., and Dhuime, B., 2019, Rates of generation and growth of the continental crust: Geoscience Frontiers, v. 10, p. 165–173, https://doi.org/10.1016/j.gsf.2018.02.004.

Hayes, B., Bédard, J.H., Hryciuk, M., Wing, B., Nabelek, P., MacDonald, W.D., and Lissenberg, C.J., 2015, Sulfide immiscibility induced by wall-rock assimilation in a fault-guided basaltic feeder system, Franklin large igneous province, Victoria Island (Arctic Canada): Economic Geology and the Bulletin of the Society of Economic Geologists, v. 110, p. 1697–1717, https://doi.org/10.2113/econgeo.110.7.1697.

Heinonen, A.P., Andersen, T., and Rämö, O.T., 2010, Re-evaluation of rapakivi petrogenesis: Source constraints from the Hf isotope composition of zircon in the rapakivi granites and associated mafic rocks of southern Finland: Journal of Petrology, v. 51, p. 1687–1709, https://doi.org/10.1093/petrology/egq035.

Hirschmann, M.M., Ghiorso, M.S., Wasylenki, L.E., Asimow, P.D., and Stolper, E.M., 1998, Calculation of peridotite partial melting from thermodynamic models of minerals and melts: I. Review of methods and comparison with experiments: Journal of Petrology, v. 39, p. 1091–1115, https://doi.org/10.1093/petroj/39.6.1091.

Kuritani, T., Kitagawa, H., and Nakamura, E., 2005, Assimilation and fractional crystallization controlled by transport process of crustal melt: Implications from an alkali basalt–dacite suite from Rishiri Volcano, Japan: Journal of Petrology, v. 46, p. 1421–1442, https://doi.org/10.1093/petrology/egi021.

Kvassnes, A.J.S., and Grove, T.L., 2008, How partial melts of mafic lower crust affect ascending magmas at oceanic ridges: Contributions to Mineralogy and Petrology, v. 156, p. 49–71, https://doi.org/10.1007/s00410-007-0273-x.

Larsen, L.M., and Pedersen, A.K., 2009, Petrology of the Paleocene picrites and flood basalts on Disko and Nuussuaq, West Greenland: Journal of Petrology, v. 50, p. 1667–1711, https://doi.org/10.1093/petrology/egp048.

Le Bas, M.J., 2000, IUGS reclassification of the high-Mg and picritic volcanic rocks: Journal of Petrology, v. 41, p. 1467–1470, https://doi.org/10.1093/petrology/41.10.1467.

Le Bas, M.J., Le Maitre, R.W., Streckeisen, A., and Zanettin, B.A., 1986, Chemical classification of volcanic rocks based on the total alkali-silica diagram: Journal of Petrology, v. 27, p. 745–750, https://doi.org/10.1093/petrology/27.3.745.

Lightfoot, P.C., Naldrett, A.J., Gorbachev, N.S., Doherty, W., and Fedorenko, V.A., 1990, Geochemistry of the Siberian Trap of the Noril'sk area, USSR, with implications for the relative contributions of crust and mantle to flood basalt magmatism: Contributions to Mineralogy and Petrology, v. 104, p. 631–644, https://doi.org/10.1007/BF01167284.

Moore, N.E., Grunder, A.L., Bohrson, W.A., Carlson, R.W., and Bindeman, I.N., 2020, Changing mantle sources and the effects of crustal passage on the Steens Basalt, SE Oregon: Chemical and isotopic constraints: Geochemistry Geophysics Geosystems, v. 21, e2020GC008910. https://doi.org/10.1029/2020GC008910.

Pamukcu, A.S., Gualda, G.A.R., Ghiorso, M.S., Miller, C.F., and McCracken, R.G., 2015, Phase-equilibrium geobarometers for silicic rocks based on rhyolite-MELTS—Part 3: Application to the Peach Spring Tuff (Arizona-California-Nevada, USA): Contributions to Mineralogy and Petrology, v. 169, 33, https://doi.org/10.1007/s00410-015-1122-y.

Pearce, J.A., and Reagan, M.K., 2019, Identification, classification, and interpretation of boninites from Anthropocene to Eoarchean using Si-Mg-Ti systematics: Geosphere, v. 15, p. 1008–1037, https://doi.org/10.1130/GES01661.1.

Pichavant, M., Weber, C., and Villaros, A., 2019, Effect of anorthite on granite phase relations: Experimental data and models: Comptes Rendus Geoscience, v. 351, p. 540–550, https://doi.org/10.1016/j.crte.2019.10.001.

Rivera, M., Martin, H., Le Pennec, J.-L., Thouret, J.-C., Gourgaud, A., and Gerbe, M.-C., 2017, Petro-geochemical constraints on the source and evolution of magmas at El Misti volcano, Peru: Lithos, v. 268-271, p. 240−259. https://doi.org/10.1016/j.lithos.2016.11.009.

Rudnick, R.L., and Gao, S., 2003, Composition of the continental crust, in, Rudnick, R.L., ed., Treatise on Geochemistry, Volume 3: The Crust: Oxford, UK, Elsevier-Pergamon, p. 1−64. https://doi.org/10.1016/B0-08-043751-6/03016-4.

Samalens, N., Barnes, S.-J., and Sawyer, E.W., 2017, The role of black shales as a source of sulfur and semimetals in magmatic nickel-copper deposits: Example from the Partridge River Intrusion, Duluth Complex, Minnesota, USA: Ore Geology Reviews, v. 81, p. 173–187, https://doi.org/10.1016/j.oregeorev.2016.09.030.

Sparks, R.S.J., 1986, The role of crustal contamination in magma evolution through geological time: Earth and Planetary Science Letters, v. 78, p. 211–223, https://doi.org/10.1016/0012-821X(86)90062-2.

Thompson, A.B., Matile, L., and Ulmer, P., 2002, Some thermal constraints on crustal assimilation during fractionation of hydrous, mantle-derived magmas with examples from central Alpine batholiths: Journal of Petrology, v. 43, p. 403–422, https://doi.org/10.1093/petrology/43.3.403.

Trial, A.F., and Spera, F.J., 1990, Mechanisms for the generation of compositional heterogeneities in magma chambers: Geological Society of America Bulletin, v. 102, p. 353–367, https://doi.org/10.1130/0016-7606(1990)102<0353:MFTGOC>2.3.CO;2.

Printed in USA